BIT ERROR RATE MINIMIZING CHANNEL SHORTENING EQUALIZERS FOR MULTICARRIER SYSTEMS

Richard K. Martin[*] *Koen Vanbleu* *Geert Ysebaert* *Andrew G. Klein*[†]

The Air Force Inst. of Tech. Broadcom Corporation Alcatel Bell Supélec
Dept. of ECE Mechelen Antwerpen Gif-sur-Yvette
WPAFB, OH, 45433 Belgium Belgium France
richard.martin koen.vanbleu geert.ysebaert agk5
@afit.edu @broadcom.com @alcatel.be @cornell.edu

ABSTRACT

Multicarrier systems first became widely used for digital subscriber lines (DSL). In DSL, the performance metric is the bit rate that can be provided without exceeding a given bit error rate (BER). Wireless multicarrier systems are becoming more popular, and in such systems the appropriate performance metric is the BER for a given bit rate. Multicarrier systems are robust to multipath provided that the channel delay spread is shorter than the guard interval between blocks. If this condition is not met, a channel shortening equalizer can be used. Previous work on channel shortening has focussed on maximizing the bit rate for DSL. We propose and evaluate a channel shortener that attempts to directly minimize the BER of a wireless multicarrier system.

1. INTRODUCTION

There are two types of multicarrier modulation. In in wireline systems, it is called discrete multitone (DMT), and wireless systems, it is called orthogonal frequency division multiplexing (OFDM). Examples of wireline multicarrier systems include power line communications (HomePlug) and digital subscriber lines (DSL). Examples of wireless multicarrier systems include wireless local area networks (IEEE 802.11a/g, HIPERLAN/2, MMAC), wireless metropolitan area networks (IEEE 802.16), digital video and audio broadcasting in Europe, satellite radio (Sirius and XM Radio), and multiband ultra wideband (IEEE 802.15.3a).

Multicarrier modulation is robust to multipath, provided that the delay spread of the transmission channel is less than the length of the cyclic prefix (CP) between transmitted blocks. If the channel is short, then equalization of the channel can be done point-wise in the frequency domain by a bank of complex scalars, called a frequency-domain equalizer (FEQ). However, if the channel is longer than the CP, additional equalization is required. Typically, this takes the form of a channel shortening equalizer (CSE) [a.k.a. a time-domain equalizer (TEQ)]. A survey of CSE design for DSL can be found in [1].

Channel shortening was first applied to maximum likelihood sequence estimation [2]. More recently, it has been used to shorten the long wireline impulse responses encountered by DSL [3], [4]. While early designs were based on heuristic cost functions, more recent designs have focussed on maximizing the bit rate for a given bit error rate [5], [6], [7], which is the appropriate measurement of performance in wireline multicarrier systems that allow bit allocation.

Wireless multicarrier systems generally have a fixed bit allocation, and receiver performance is measured in terms of bit error rate (BER). Moreover, in wireline systems, once bit allocation has been done, the CSE can be used to minimize the BER of that bit allocation. To date, no CSE design in the literature explicitly minimizes the BER. Hence, the main goals of this paper are to investigate the BER cost surface for multicarrier systems, and to develop and assess a CSE that minimizes the BER.

2. SYSTEM MODEL

We assume a multiple-input multiple-output (MIMO) channel model with L transmit antennas and P receive antennas. Throughout, $(\cdot)^*$, $(\cdot)^T$, and $(\cdot)^H$ denote complex conjugate, matrix transpose, and conjugate transpose, respectively, and $\mathcal{E}\{\cdot\}$ denotes statistical expectation. The notation was chosen to be consistent with [8].

The system model is shown in Fig. 1. We assume that N_a of the N tones are active; for example, in popular wireless LANs, $N = 64$, but only $N_a = 52$ tones are used. The set of active tones is denoted $\mathcal{S}_a$. The data symbols (usu-

[*]Funded by the Air Force Office of Scientific Research. The views expressed in this paper are those of the authors, and do not reflect the official policy or position of the United States Air Force, Department of Defense, or the U.S. Government. This document has been approved for public release; distribution unlimited.

[†]Supported by a Chateaubriand Scientific Postdoctoral Fellowship.

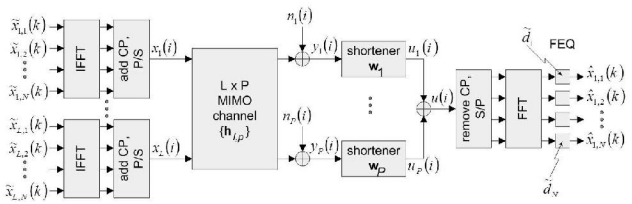

Fig. 1. Complex baseband multicarrier system model.

ally multi-level QAM) are blocked into groups of size N_a and zero-padded to length N. The k^{th} such block for transmitter l is denoted $\widetilde{\mathbf{x}}_l(k)$. Then an inverse discrete Fourier transform (IDFT), implemented by the fast Fourier transform (FFT), is taken to get N time-domain samples. We use $\mathcal{F}$ to denote the unitary $N \times N$ matrix that computes the DFT, with element (m, n) given by $(1/\sqrt{N})e^{-\jmath 2\pi mn/N}$. A cyclic prefix is appended by copying the last ν samples of the block to the beginning of the block, and then the $S = N + \nu$ samples are transmitted serially. The i^{th} transmitted data sample is denoted $x_l(i)$. Note that l indexes the transmit antenna, p indexes the receive antenna, k is the block index, n is the tone index, i is the sample index, and $\jmath = \sqrt{-1}$ is the unit imaginary number.

The presence of the CP is represented by

$$x_l\left(Sk+i\right) = x_l\left(Sk+i+N\right), \qquad (1)$$
$$1 \le l \le L, \quad 1 \le i \le \nu, \quad -\infty < k < \infty.$$

Let $\mathbf{h}_{l,p}$ be an FIR filter of length L_h, which models the channel from transmit antenna l to receive antenna p, and let $\mathbf{w}_p$ be an FIR filter of length L_w, which is the CSE to be designed for antenna p. Let $\mathbf{H}_{l,p}$ be the tall channel convolution matrix for $\mathbf{h}_{l,p}$, which is an $L_c \times L_w$ Toeplitz matrix, where $L_c = L_h + L_w - 1$.

Define the transmitted signal vectors

$$\mathbf{x}_l(i) = \left[x_l(i), \cdots, x_l(i - L_c + 1)\right]^T, \qquad (2)$$
$$\mathbf{x}(i) = \left[\mathbf{x}_1^T(i), \cdots, \mathbf{x}_L^T(i)\right]^T, \qquad (3)$$

and similarly for $\boldsymbol{\eta}_p(i)$, $\boldsymbol{\eta}(i)$, $\mathbf{y}_p(i)$, $\mathbf{y}(i)$. We can compactly write the CSE input vector as

$$\mathbf{y}(i) = \begin{bmatrix} \mathbf{H}_{1,1}^T, & \cdots, & \mathbf{H}_{L,1}^T \\ \vdots & \ddots & \vdots \\ \mathbf{H}_{1,P}^T, & \cdots, & \mathbf{H}_{L,P}^T \end{bmatrix} \mathbf{x}(i) + \boldsymbol{\eta}(i). \qquad (4)$$

The input to the DFT at the receiver is then obtained by passing the signal through the bank of CSEs,

$$u(i) = \underbrace{\left[\mathbf{w}_1^T, \cdots, \mathbf{w}_P^T\right]}_{\mathbf{w}^T} \mathbf{y}(i). \qquad (5)$$

After channel shortening, the cyclic prefix is removed from each block and a DFT is applied. This requires an estimate of the transmission delay Δ, since the length N DFT input vector for block k is

$$\mathbf{u}(k) = \left[u(Sk+\nu+1+\Delta), \cdots, u(S(k+1)+\Delta)\right]^T. \qquad (6)$$

The delay Δ is a design parameter whose choice affects the values of the optimal CSE as well as the performance that can be attained. After the DFT, the FEQ input vector is

$$\widetilde{\mathbf{u}}(k) = \mathcal{F}\,\mathbf{u}(k). \qquad (7)$$

Finally, the FEQ is used to invert the channel in the frequency domain to estimate the data. Without loss of generality, we assume that the receiver is attempting to recover the data from transmitter $l = 1$. Thus, the FEQ output is

$$\widehat{\mathbf{x}}_1(k) = \widetilde{\mathbf{d}}_o \odot \widetilde{\mathbf{u}}(k), \qquad (8)$$

where $\odot$ denotes element-by-element multiplication; and $\widetilde{\mathbf{d}}_o$ contains the FEQ $\widetilde{\mathbf{d}}$, a bank of N_a complex scalars, zero-padded to length N. In a multiuser scheme, the data for $l = 2, \cdots, L$ can be ignored, or multi-user detection can be used to mitigate the interference. For a single user, $\widetilde{x}_l$ may be the same on all transmitters l, or an Alamouti-type code may be used [9].

3. BER MODELS

The goal of this section is to derive a model for the BER of a multicarrier system. In Section 3.1, we will model the BER for a multicarrier system in terms of the effective output SNR on the various subchannels, in Section 3.2 we will review the subchannel SNR model for multicarrier systems in [8] and extend it to the MIMO case.

3.1. The multicarrier BER model

We assume that the total residual interference and noise at the output of each tone is Gaussian, and that M-level QAM signalling (consisting of two orthogonal $\sqrt{M}$-level PAM signals) is used on each tone. Common wireless LAN standards support 4-QAM, 16-QAM, and 64-QAM. The probability of error on each of the PAM components is given by [10, pp.225–226]

$$P_{\sqrt{M}}(n) = 2\left(1 - \frac{1}{\sqrt{M}}\right) Q\left(\sqrt{\frac{3}{M-1}\mathrm{SNR}_n}\right), \qquad (9)$$

hence the symbol error rate (SER) on tone n is

$$P_M(n) = 2P_{\sqrt{M}}(n) - \left(P_{\sqrt{M}}(n)\right)^2, \qquad (10)$$

where SNR_n is the effective signal-to-interference-and-noise ratio on tone n (usually called the subchannel SNR); and

$Q(x)$ is the integral of a unit Gaussian PDF from x to infinity. For the $M = 4$ case, (9) is the BER for tone n, and it reduces to $Q\left(\sqrt{\text{SNR}_n}\right)$, which we use here for simplicity. Averaging (9) and (10) over the active tones, the BER and the SER for the output of an OFDM system with $M = 4$ are

$$BER = \frac{1}{N_a} \sum_{n \in \mathcal{S}_a} Q\left(\sqrt{\text{SNR}_n}\right), \tag{11}$$

$$SER = \frac{1}{N_a} \sum_{n \in \mathcal{S}_a} \left(2Q\left(\sqrt{\text{SNR}_n}\right) - Q^2\left(\sqrt{\text{SNR}_n}\right)\right). \tag{12}$$

Either can be used as the objective function to be minimized; we will choose the BER. For comparison, the BM design [8] uses the objective function

$$b = \sum_{n \in \mathcal{S}_a} \log_2\left(1 + \frac{\text{SNR}_n}{\Gamma}\right), \tag{13}$$

where $\Gamma = 19.1$ (or 12.8 dB). In the next section, we model the subchannel SNR in terms of the CSE coefficients.

3.2. The multicarrier subchannel SNR model

The subchannel SNR can be modelled in various ways [3], [5], [6], [7], [8], [11]. Most models take the form

$$\text{SNR}_n = \frac{\mathbf{w}^H \mathbf{B}_n \mathbf{w}}{\mathbf{w}^H \mathbf{A}_n \mathbf{w}}, \tag{14}$$

where $\mathbf{A}_n$ and $\mathbf{B}_n$ are Hermitian positive semi-definite matrices. The distinction between models lies in how the inter-carrier/intersymbol interference (ICI/ISI) and DFT leakage are taken into account. In this section, we review the subchannel SNR model of [7], [8], although in the more general context of a MIMO channel model.

The DFT output can be written as

$$\mathcal{F}\underbrace{(\mathbf{Y}_k \mathbf{w})}_{\mathbf{u}(k)} = \underbrace{(\mathcal{F}\mathbf{Y}_k)}_{\widetilde{\mathbf{Y}}_{k,N}} \mathbf{w}, \tag{15}$$

where $\mathbf{Y}_k$ is a block Toeplitz matrix of size $N \times (PL_w)$, where each $N \times L_w$ sub-block contains the data that will be convolved with the p^{th} CSE, $\mathbf{w}_p$, and successive rows are vectors $\mathbf{y}^T(i)$ for successive values of i. Then $\widetilde{\mathbf{Y}}_{k,N}$ is an $N \times (PL_w)$ matrix as well, with n^{th} the row denoted by $\widetilde{\mathbf{y}}_{k,n}$. As in [8], define the correlation terms (still assuming that the user of interest is $l = 1$)

$$\sigma_n^2 \triangleq \mathcal{E}\left\{\left|\widetilde{\mathbf{x}}_1^*(k)[n]\right|^2\right\}, \tag{16}$$

$$\boldsymbol{\varphi}_n \triangleq \mathcal{E}\left\{\widetilde{\mathbf{x}}_1^*(k)[n]\widetilde{\mathbf{y}}_{k,n}\right\}, \tag{17}$$

$$\boldsymbol{\Sigma}_n^2 \triangleq \mathcal{E}\left\{\widetilde{\mathbf{y}}_{k,n}^H \widetilde{\mathbf{y}}_{k,n}\right\}, \tag{18}$$

of dimensions 1×1, $1 \times PL_w$, and $PL_w \times PL_w$, respectively.

If the SNR is measured at the output of the FEQ, then the desired signal is an undistorted version of the signal. Then the subchannel SNR on tone n is the ratio of the power of the desired signal, $\widetilde{\mathbf{x}}_1(k)[n]$, to the power of the error signal, $\widetilde{e}_{k,n} = \widetilde{d}_n \widetilde{\mathbf{y}}_{k,n}\mathbf{w} - \widetilde{\mathbf{x}}_1(k)[n]$, and is given by

$$\begin{aligned}\text{SNR}_n &= \frac{\sigma_n^2}{\mathcal{E}\left\{\left|\widetilde{e}_{k,n}\right|^2\right\}} = \frac{\sigma_n^2}{\mathcal{E}\left\{\left|\widetilde{d}_n \widetilde{\mathbf{y}}_{k,n}\mathbf{w} - \widetilde{\mathbf{x}}_1(k)[n]\right|^2\right\}} \\ &= \frac{\sigma_n^2}{\left|\widetilde{d}_n\right|^2 \mathbf{w}^H \boldsymbol{\Sigma}_n^2 \mathbf{w} - \widetilde{d}_n \boldsymbol{\varphi}_n \mathbf{w} - \widetilde{d}_n^* \boldsymbol{\varphi}_n^* \mathbf{w}^* + \sigma_n^2}.\end{aligned} \tag{19}$$

The unbiased MMSE FEQ for tone n is found by setting the correlation of the input and output on tone n equal to the transmitted power on tone n [8], and is thus given by

$$\widetilde{d}_n^{\text{uMMSE}} = \frac{\sigma_n^2}{\boldsymbol{\varphi}_n \mathbf{w}}. \tag{20}$$

Substituting the FEQ (20) into the subchannel SNR model (19) yields (14) with

$$\mathbf{A}_n = \sigma_n^2 \boldsymbol{\Sigma}_n^2 - \boldsymbol{\varphi}_n^H \boldsymbol{\varphi}_n, \tag{21}$$

$$\mathbf{B}_n = \boldsymbol{\varphi}_n^H \boldsymbol{\varphi}_n. \tag{22}$$

The auto- and cross-correlations can be empirically estimated, assuming sufficient training data is available.

To visualize the model of the BER of (11), consider the channel $\mathbf{h} = [1, -0.3, 0.7]$, with a CP length of $\nu = 1$, so that we wish to shorten the channel to length 2. A 3-tap CSE under a unit norm constraint (which does not affect the BER) can be parameterized by the two angles of spherical coordinates. Fig. 2 shows log-spaced contours of the BER. The FFT size was $N = 8$, and the SNR was 20 dB. Observe that the BER is multimodal even for this low-dimensional example.

The case of no CSE (or a CSE of $\mathbf{w} = [1, 0, 0]$) is shown as a dot, the maximum shortening SNR (MSSNR) CSE [4] is shown as a square, and the CSE that minimizes the BER is shown as a circle. Here, the MSSNR CSE actually degrades the BER relative to no CSE, although this is not always the case.

4. BER MINIMIZATION ALGORITHMS

In this section, we present an iteratively reweighted (IR) minimum error rate (MER) algorithm, and a Gauss-Newton (GN) update rule that has better convergence properties. The development parallels the development of the IR and GN designs in [8] which maximize the bit rate for systems that allow bit allocation across the tones.

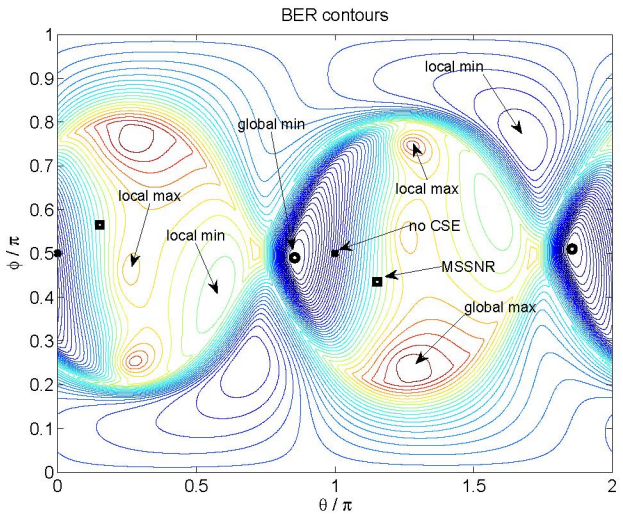

Fig. 2. Contours of the BER for a 3-tap CSE under a unit norm constraint. The CSE is parameterized in spherical coordinates by the angles θ and ϕ. The cost function is symmetric with respect to a sign change in the CSE ($\mathbf{w} \rightarrow -\mathbf{w}$), which corresponds to $(\theta, \phi) \rightarrow (\theta + \pi, \pi - \phi)$, hence only half of the critical points are labelled.

4.1. Iterative update rule

We wish to minimize the objective function (11) with respect to the parameter vector $\boldsymbol{\theta} = [\mathbf{w}^T, \widetilde{\mathbf{d}}^T]^T$, subject to the constraint of (20). Since minimization of a function is not affected by scaling the function, we will ignore the leading factor of $1/N_a$. A constrained minimization problem can be transformed into an unconstrained minimization problem by adding a Lagrangian term,

$$J_L = \sum_{n \in \mathcal{S}_a} \left[Q\left(\sqrt{\text{SNR}_n}\right) - \mathcal{R}\left\{ \lambda_n^* \left(\widetilde{d}_n \boldsymbol{\varphi}_n \mathbf{w} - \sigma_n^2 \right) \right\} \right], \tag{23}$$

where the N_a scalars λ_n are Lagrange multipliers, and the real operator $\mathcal{R}\{\cdot\}$ ensures a real constraint term. The procedure we will use to derive the IR update rule is:

1. Set the gradient of (23) with respect to $\widetilde{d}_n$ equal to zero, $\nabla_{\widetilde{d}_n} J_L = 0$, and use the result along with the constraint on $\widetilde{d}_n$ to solve for λ_n.
2. Compute the gradient of (23) with respect to $\boldsymbol{\theta}$, then substitute in the values of λ_n.
3. Set the gradient to zero, which gives an equation that will be satisfied by the BER-minimizing CSE.
4. Replace the expectation with a time average and replace the equality with a least-squares minimization.
5. Iteratively solve this minimization problem in the manner of Section II.D of [8].

After estimating the correlation terms σ_n^2, $\boldsymbol{\varphi}_n$, and $\boldsymbol{\Sigma}_n^2$ in (16), (17), and (18) from time averages, loop through:

1. Estimate the weights $\check{\gamma}_n$ based on the previous value of the CSE:
   $\rho^{-2} = \frac{\sigma_n^2 \mathbf{w}^H \boldsymbol{\Sigma}_n^2 \mathbf{w}}{\mathbf{w}^H \boldsymbol{\varphi}_n^H \boldsymbol{\varphi}_n \mathbf{w}}$
   $\text{SNR}_n = \frac{1}{\rho^{-2} - 1}$
   $\check{\gamma}_n = \frac{\left(1+\text{SNR}_n\right)^2}{\text{SNR}_n^2} \gamma_n = \frac{e^{-(\text{SNR}_n)/2}}{\sqrt{2\pi}\sqrt{\text{SNR}_n}} \cdot \frac{\left(1+\text{SNR}_n\right)^2}{\sigma_n^2}$
2. Compute the LS estimate of the biased MMSE FEQ
   $\widetilde{d}_n = \frac{\mathbf{w}^H \boldsymbol{\varphi}_n^H}{\mathbf{w}^H \boldsymbol{\Sigma}_n^2 \mathbf{w}}$
3. Compute the LS estimate of the new CSE:
   $\mathbf{w} = \left\{ \sum_{n \in \mathcal{S}_a} \check{\gamma}_n \left| \widetilde{d}_n \right|^2 \boldsymbol{\Sigma}_n^2 \right\}^{-1} \left\{ \sum_{n \in \mathcal{S}_a} \check{\gamma}_n \widetilde{d}_n^* \boldsymbol{\varphi}_n^H \right\}$

Fig. 3. Iteratively reweighted minimum error rate (IR-MER) CSE design algorithm.

For step 1, the element of the gradient from the n^{th} FEQ parameter is

$$\nabla_{\widetilde{d}_n} J_L = \underbrace{\frac{1}{\sqrt{2\pi}} \frac{e^{(-\text{SNR}_n)/2}}{\sqrt{\text{SNR}_n}} \cdot \frac{\text{SNR}_n^2}{\sigma_n^2}}_{\gamma_n} \mathcal{E}\left\{ \widetilde{\mathbf{y}}_{k,n}^* \mathbf{w}^* \widetilde{e}_{k,n} \right\} - \lambda_n \mathcal{E}\left\{ \widetilde{\mathbf{y}}_{k,n}^* \mathbf{w}^* \widetilde{x}_{k,n} \right\}, \tag{24}$$

which equals zero at the location of a minimum. Note that this derivative is very similar to the corresponding eq. (66) in [8], with the only difference being how γ_n is defined. With this redefinition of γ_n, the rest of the algorithm development is similar to that in [8]. Thus, for space considerations, we simply outline the resulting algorithm in Fig. 3.

4.2. Gauss-Newton update rule

The IR-MER CSE converges only linearly, and this can be increased via an iterative Gauss-Newton algorithm. Such an algorithm is a gradient descent algorithm, but the direction of the update vector is adjusted by the inverse of the Hessian of the cost function:

$$\boldsymbol{\theta}_{i+1} = \boldsymbol{\theta}_i - \mu_i \left(\nabla_{\boldsymbol{\theta}}^2 J \right)^{-1} \nabla_{\boldsymbol{\theta}} J \Big|_{\boldsymbol{\theta}_i} \tag{25}$$

Again, with the redefinition of the weights γ_n, the algorithm development is similar to that in [8]. Thus, for space considerations, we simply outline the resulting algorithm in Fig. 4.

5. SIMULATIONS

Consider a wireless system with FFT size $N = 64$, CP length $\nu = 16$, and $N_a = 52$ active tones (hence 12 null

After estimating the correlation terms σ_n^2, $\boldsymbol{\varphi}_n$, and $\boldsymbol{\Sigma}_n^2$ in (16), (17), and (18) from time averages, loop through:

1. Same as Fig. 3.
2. Same as Fig. 3.
3. Compute the following:
   $\mathbf{E}_{\tilde{\mathbf{d}}} = \sum_{n\in\mathcal{S}_a} \check{\gamma}_n \left|\widetilde{d}_n\right|^2 \boldsymbol{\Sigma}_n^2$
   $\mathbf{F}_{\boldsymbol{\theta}} = \left[\cdots \quad \left[\check{\gamma}_n^* \widetilde{d}_n^* \left(\boldsymbol{\Sigma}_n^2 \mathbf{w}\right)\right] \quad \cdots\right]$
   $\mathbf{G}_{\mathbf{w},D} = \text{diag}\left[\cdots \check{\gamma}_n \left(\mathbf{w}^H \boldsymbol{\Sigma}_n^2 \mathbf{w}\right) \cdots\right]$
   $\mathbf{Q}_{\boldsymbol{\theta}} = \mathbf{E}_{\tilde{\mathbf{d}}} - \mathbf{F}_{\boldsymbol{\theta}} \mathbf{G}_{\mathbf{w},D}^{-1} \mathbf{F}_{\boldsymbol{\theta}}^H$
   $\nabla_{\mathbf{w}} J = \sum_{n\in\mathcal{S}_a} \check{\gamma}_n \widetilde{d}_n^* \left(\widetilde{d}_n \boldsymbol{\Sigma}_n^2 \mathbf{w} - \boldsymbol{\varphi}_n^H\right)$
4. For a small step size μ, compute the new CSE:
   $\mathbf{w}_{new} = \mathbf{w}_{old} - \mu\, \mathbf{Q}_{\boldsymbol{\theta}}^{-1} \left(\nabla_{\mathbf{w}} J\right)$
5. Renormalize the CSE:
   $\mathbf{w}_{new} = \mathbf{w}_{new} / \|\mathbf{w}_{new}\|$

Fig. 4. Gauss-Newton minimum error rate (GN-MER) CSE design algorithm.

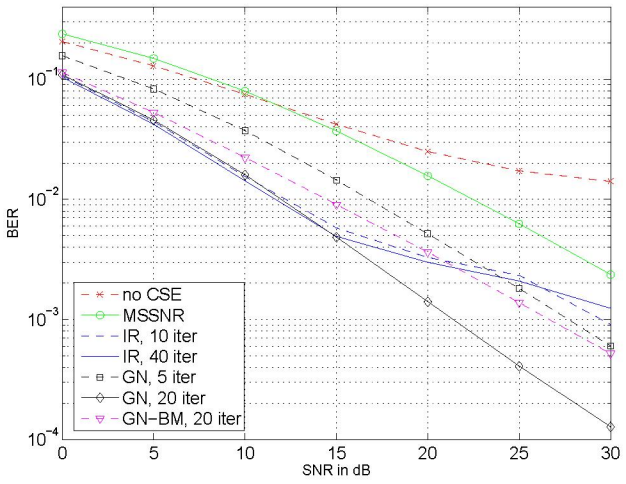

Fig. 5. Bit error rate vs. SNR for various CSE designs.

tones), as in popular wireless LAN standards. The channels are Rayleigh fading with 32 taps, using the delay profile of [12]. We assume $L = 1$ transmit antenna and $P = 2$ receive antennas. The correlation parameters σ_n^2, $\boldsymbol{\varphi}_n$, and $\boldsymbol{\Sigma}_n^2$ were estimated using 1000 symbols of training. The results will be averaged over 250 independently generated channels, data, and noise sequences.

Fig. 5 shows the BER versus SNR. The designs considered are no CSE, an MSSNR CSE, the proposed IR-MER CSE, the proposed GN-MER CSE, and the GN-BM design of [8]. The MSSNR CSE was used to initialize the IR and GN algorithms. The proposed IR and GN algorithms outperform all of the others, including the GN-BM algorithm, although the IR algorithm does not do as well as the GN at high SNR values.

6. REFERENCES

[1] R. K. Martin, K. Vanbleu, M. Ding, G. Ysebaert, M. Milosevic, B. L. Evans, M. Moonen, and C. R. Johnson, Jr., "Unification and Evaluation of Equalization Structures and Design Algorithms for Discrete Multitone Modulation Systems," *IEEE Trans. on Signal Processing*, vol. 53, no. 10, pp. 3880–3894, Oct. 2005.

[2] D. D. Falconer and F. R. Magee, "Adaptive Channel Memory Truncation for Maximum Likelihood Sequence Estimation," *Bell Sys. Tech. Journal*, pp. 1541–1562, Nov. 1973.

[3] N. Al-Dhahir and J. M. Cioffi, "Optimum Finite-Length Equalization for Multicarrier Transceivers," *IEEE Trans. on Comm.*, vol. 44, no. 1, pp. 56–64, Jan. 1996.

[4] P. J. W. Melsa, R. C. Younce, and C. E. Rohrs, "Impulse Response Shortening for Discrete Multitone Transceivers," *IEEE Trans. on Comm.*, vol. 44, pp. 1662–1672, Dec. 1996.

[5] G. Arslan, B. L. Evans, and S. Kiaei, "Equalization for Discrete Multitone Receivers To Maximize Bit Rate," *IEEE Trans. on Signal Processing*, vol. 49, no. 12, pp. 3123–3135, Dec. 2001.

[6] M. Milosevic, L. F. C. Pessoa, B. L. Evans, and R. Baldick, "DMT Bit Rate Maximization with Optimal Time Domain Equalizer Filter Bank Architecture," in *Proc. IEEE Asilomar Conf. on Signals, Systems, and Comp.*, Pacific Grove, CA, Nov. 2002, vol. 1, pp. 377–382.

[7] K. Vanbleu, G. Ysebaert, G. Cuypers, M. Moonen, and K. Van Acker, "Bitrate Maximizing Time-Domain Equalizer Design for DMT-based Systems," *IEEE Trans. on Comm.*, vol. 52, no. 6, pp. 871–876, June 2004.

[8] K. Vanbleu, G. Ysebaert, G. Cuypers, and M. Moonen, "On Time-Domain and Frequency-Domain MMSE-Based TEQ Design for DMT Transmission," *IEEE Trans. Signal Processing*, vol. 53, no. 8, pp. 3311–3324, Aug. 2005.

[9] S. M. Alamouti, "A Simple Transmit Diversity Technique for Wireless Communications," *IEEE Journal on Selected Areas in Comm.*, vol. 16, pp. 1451–1458, Oct. 1998.

[10] G. L. Stuber, *Principles of Mobile Communication*, Kluwer Academic Publishers, Boston, 1996.

[11] W. Henkel and T. Kessler, "Maximizing the Channel Capacity of Multicarrier Transmission by Suitable Adaptation of the Time-domain Equalizer," *IEEE Trans. on Comm.*, vol. 48, no. 12, pp. 2000–2004, Dec. 2000.

[12] R. K. Martin, J. M. Walsh, and C. R. Johnson, Jr., "Low Complexity MIMO Blind, Adaptive Channel Shortening," *IEEE Trans. on Signal Processing*, vol. 53, no. 4, pp. 1324–1334, Apr. 2005.